The Astrophysical Journal, 634:436–441, 2005 November 20

SIMBA OBSERVATIONS OF THE KEYHOLE NEBULA

Kate J. Brooks[1]
Australia Telescope National Facility, P.O. Box 76, Epping NSW 1710, Australia

Guido Garay
Departamento de Astronomía, Universidad de Chile, Casilla 36-D, Santiago, Chile

Markus Nielbock
Astronomisches Institut der Ruhr-Universität Bochum, Universitätsstraße 150, D-44780 Bochum, Germany

Nathan Smith
Center for Astrophysics and Space Astronomy, University of Colorado, 389 UCB, Boulder, CO 80309

and

Pierre Cox
Institut de RadioAstronomie Millimétrique, 300 rue de la Piscine, Domaine Universitaire, 38406 Saint Martin d'Hres, France
Received 2005 May 10; accepted 2005 August 2

ABSTRACT

We report observations made with the SIMBA bolometer at SEST to measure the 1.2 mm continuum emission toward the Keyhole nebula. We have detected 1.2 mm emission toward the ionized gas filaments of the Car II radio source that is attributed to thermal free-free emission. Several compact 1.2 mm emission sources have also been identified and found to correspond to bright-rimmed molecular globules. Under the assumption that for these sources the 1.2 mm emission corresponds to dust, we find mass estimates in the range 3–19 $M_{\odot}$, which are consistent with previous molecular line measurements. The data also yield new 1.2 mm flux measurements at two different epochs during the cyclic brightness variation of η Carinae. No emission was detected toward the trademark dark keyhole of the nebula, consistent with it being cool molecular gas situated at the outskirts of the H II region.

Subject headings: dust, extinction — H II regions — ISM: individual (Keyhole Nebula) — radio continuum: ISM — stars: individual (η Carinae)

1. INTRODUCTION

The fast stellar winds and strong ionizing radiation from a cluster of young massive stars have a profound impact on the giant molecular cloud (GMC) from which they form. Ultimately, the massive stars will ionize the gas and destroy the GMC but not before drastically changing its internal structure and chemistry and possibly triggering further star formation. The Keyhole Nebula is a prime target for the study of such fierce processes in action.

The Keyhole nebula is part of the Carina nebula (NGC 3372), an H II region/GMC complex at a distance of ≈2.2 kpc (see, e.g., Allen & Hillier 1993). The Carina GMC extends over 130 pc with a total mass in excess of 5×10^5 $M_{\odot}$ (e.g., Brooks et al. 1998) and appears to have been swept up by a young bipolar superbubble that is beginning to break out of the Galactic plane (Smith et al. 2000). The spectacular appearance of the Keyhole nebula at optical wavelengths has made it the most famous part of the Carina nebula. Located near the center of the Carina nebula, it is exposed to the harsh radiation fields and stellar winds from the nearby massive stellar members of Trumpler 16 (Tr 16) and one of the most massive stars known—η Carinae (η Car). Associated with the Keyhole nebula are bright optical emission filaments and obscuring dust, which have conspired to form the shape of an old-fashioned keyhole (hence the name "Keyhole nebula"). The optical emission filaments of the Keyhole nebula are associated with strong radio continuum emission that was first detected by Gardner & Morimoto (1968) and named Car II. The reflected spectrum of η Car is seen throughout Car II, establishing that the two are indeed at the same distance (Walborn & Liller 1977; López & Meaburn 1986).

In this paper we report observations made with the SIMBA bolometer at the Swedish-European Submillimeter Telescope (SEST) to measure the 1.2 mm continuum emission associated with the Keyhole nebula. This work is part of a larger 1.2 mm continuum survey of the entire Carina nebula to identify sites for the next generation of star formation.

2. OBSERVATIONS

Observations were made using the SIMBA bolometer installed on the SEST at the European Southern Observatory, La Silla, Chile. SIMBA is a 37 channel hexagonal array operating at a wavelength of 1.2 mm (250 GHz). At this wavelength, the half-power beamwidth (HPBW) of the SEST telescope is 24″. Each array element has a bandwidth of approximately 90 GHz and a separation on the sky of 44″. Data were obtained over two periods, 2001 November 2–4 and 2002 November 11–12, and without using a nutating subreflector. The average measured opacities were 0.26 and 0.17 during the 2001 and 2002 observing periods, respectively. A fast-mapping mode was used, with a scanning speed of 80″ s^{-1} and scan separation of 8″ in elevation (Reichertz et al. 2001). Each individual map covered an area of $600''\times600''$ in azimuth and elevation and took 12 minutes to complete. A series of four repeated maps were obtained toward three different pointing centers. The final image is the result of 12 co-added maps, equivalent to 144 minutes on-source observing time.

Data were edited and calibrated using the software package MOPSIC according to standard procedures described by Chini et al. (2003). A de-spiking value was set to <-5 rms with zero or

[1] For part of this work affiliated with Departamento de Astronomía, Universidad de Chile, Casilla 36-D, Santiago, Chile.

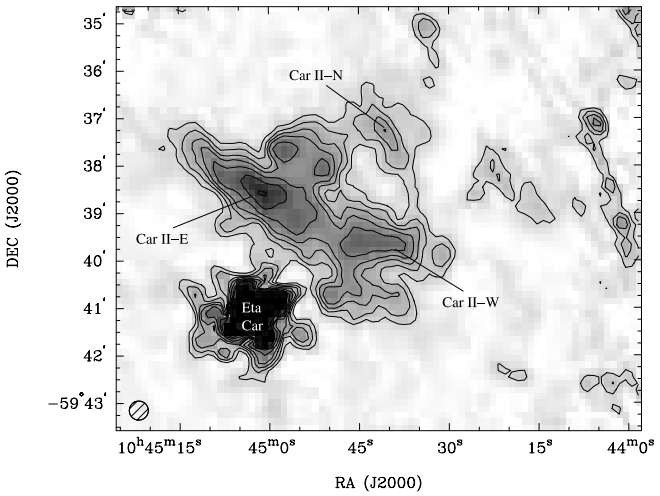

FIG. 1.—SIMBA 1.2 mm continuum emission toward the Keyhole nebula. Contour levels are 0.075 (3 σ), 0.125, 0.175, 0.225, 0.3, 0.4, 0.5, 1, 5, 10, 15, and 20 Jy beam^{-1}. The SIMBA beam size is illustrated in the lower left corner. Emission associated with η Car and the three components of the Car II radio continuum source (Car II-E, Car II-W, and Car II-N) are labeled accordingly.

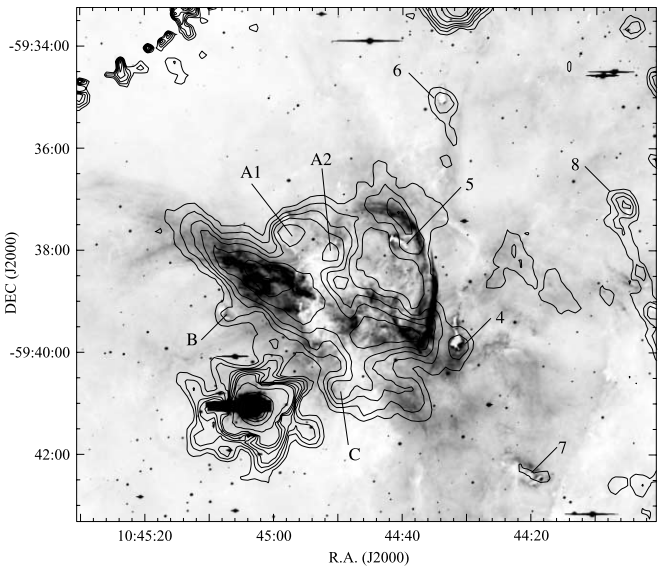

FIG. 2.—Hα emission (Smith 2002) with contours of the SIMBA 1.2 mm continuum emission (see Fig. 1). Several bright-rimmed dark globules are labeled according to their designations given by Cox & Bronfman (1995 for clumps A1, A2, 4, 5, B, and C), Smith (2002 for clump 6), and Rathborne et al. (2002 for clumps 7 and 8).

first-order baselines. The pixel size in the final image was set to 8″. Through an iterative process (set to six iterations), a preliminary image was used as a source model to improve the removal of correlated noise. Flux calibration of the data was achieved through daily observations of Uranus. The resulting multiplication factors were 0.14 and 0.062 Jy count^{-1} beam^{-1} for the 2001 and 2002 observing periods, respectively. Fluctuations between the same maps taken on different days indicate a flux uncertainty of 10%. From comparison with other data sets, we estimate that the positional uncertainty of the final image is better than 5″. The average 1 σ rms noise level in the final image is 0.015 Jy beam^{-1}.

3. RESULTS

3.1. *SIMBA* 1.2 mm *Emission*

The 1.2 mm continuum emission detected with SIMBA toward the Keyhole nebula is shown in Figure 1. Table 1 lists those sources with a 5 σ or better signal-to-noise ratio. We have adopted the naming scheme used by Smith et al. (2003a). In Figure 2 the detected 1.2 mm emission is compared to the Hα emission toward the Keyhole nebula taken from Smith (2002). Prominent in the Hα image is emission from a ring structure, which forms the Car II radio continuum source (Smith 2002; Brooks et al. 2001; Whiteoak 1994), and obscuring dust in the shape of a keyhole (hereafter referred to as the dark keyhole structure). The saturated Hα emission from η Car is easily identifiable. So too are numerous dark globules with bright rims. The detected 1.2 mm emission may be separated into three types: a very bright unresolved source associated with η Car, three elongated filaments matching the Car II emission ring, and numerous compact sources centered on the bright-rimmed globules. All of these will be discussed separately in the next section. No 1.2 mm emission was detected from the dark keyhole structure.

TABLE 1

PARAMETERS OF THE 1.2 mm CONTINUUM EMISSION CLUMPS

	PEAK POSITION							
SOURCE (1)	α (J2000.0) (2)	δ (J2000.0) (3)	PEAK FLUX (Jy beam^{-1}) (4)	FLUX DENSITY (Jy) (5)	SOURCE SIZE (arcsec × arcsec) (6)	OTHER DESIGNATIONS[a] ($M_\odot$) (7)	MASS (8)	OTHER MASS ESTIMATES[a,b] ($M_\odot$) (9)
104458.5−593739.....	10 44 58.5	−59 37 39	0.362	0.620	42 × 42	A1	19	14
104451.2−593803.....	10 44 51.2	−59 38 03	0.353	0.529	42 × 42	A2	16	
104431.2−593956.....	10 44 31.2	−59 39 56		0.152	Unresolved	4	5	6
104507.0−593915.....	10 45 07.0	−59 39 15		0.151	Unresolved	B	5	3
104450.2−594339.....	10 44 50.2	−59 40 43		0.273	Unresolved	C	8	6
104433.2−593508.....	10 44 33.2	−59 35 08		0.175	Unresolved	6	5	5–10
104417.4−594228.....	10 44 17.4	−59 42 28		0.095	Unresolved	7	3	12
104405.8−593708.....	10 44 05.8	−59 37 08	0.241	0.305	46 × 30	8	9	91
104500.7−593835.....	10 45 00.7	−59 38 35	0.508	6.00	243 × 63	Car II-E		
104444.9−593932.....	10 44 44.9	−59 39 32	0.367	2.89	113 × 63	Car II-W		
104440.6−593716.....	10 44 40.6	−59 37 16	0.229	1.25	105 × 63	Car II-N		

NOTE.—The area over which each clump was identified corresponds to the 0.075 Jy beam^{-1} (5 σ) contour level. Units of right ascension are hours, minutes, and seconds, and units of declination are degrees, arcminutes, and arcseconds.

[a] Clumps A1, A2, 4, B, and C (Cox & Bronfman 1995); clump 6 (Smith 2002); clumps 7 and 8 (Rathborne et al. 2002); Car II-N, Car II-W, and Car II-E (Whiteoak 1994).

[b] Mass estimates have all been obtained from ^{12}CO (2–1) data (Cox & Bronfman 1995; Rathborne et al. 2002) except for clump 6, which relied on absorption of the He I λ10830 line (Smith 2002).

3.2. *Mass Estimates*

There are three different emission mechanisms that can contribute to the 1.2 mm (250 GHz) continuum emission: free-free emission from ionized gas, thermal emission from dust, and ^{12}CO (2–1) line emission at 230 GHz. The frequency width of the ^{12}CO (2–1) line ($\approx$0.01 GHz) is small compared to the bandwidth of the SIMBA observations (90 GHz). We estimate that the ^{12}CO (2–1) line emission should contribute at most 1% to the total SIMBA flux density for clouds with dust temperatures of 30 K and dust opacities at 250 GHz of 0.01.

Assuming that the 1.2 mm emission is optically thin and caused mainly by thermal dust emission, the total cloud mass can be computed using the expression

$$M = 20.689\left(\frac{S_{1.2}}{\mathrm{Jy}}\right)\left(\frac{D}{\mathrm{kpc}}\right)^2\left(\frac{0.01}{R_{\mathrm{dg}}}\right) \times \left(\frac{1\ \mathrm{cm^2\ g^{-1}}}{\kappa_{1.2}}\right)\left[\exp\left(\frac{11.998}{T_d}\right) - 1\right] M_\odot \quad (1)$$

(e.g., Chini et al. 1987), where $S_{1.2}$ is the flux density measured at 1.2 mm, D is the distance, R_{dg} is the dust-to-gas ratio (taken to be 0.01), $\kappa_{1.2}$ is the dust mass absorption coefficient, and T_d is the dust temperature in K. Overall, the mass estimate can deviate from the real value by up to a factor of 10. This deviation is largely caused by the uncertainty of $\kappa_{1.2}$, which is linked to grain chemistry and morphology.

4. DISCUSSION

4.1. η *Carinae*

The strongest source detected in the SIMBA 1.2 mm data is associated with η Car. The source is unresolved by the SIMBA beam, and the starlike beam pattern of the SEST telescope is apparent at the level of $\approx$3% of the peak intensity. The flux density of η Car was taken from a two-dimensional Gaussian fit. Two separate 1.2 mm flux density measurements for η Car were obtained: 36 $\pm$ 3 Jy using the 2001 November data and 29 $\pm$ 3 Jy using the 2002 November data.

It is well established that the flux density of η Car across a wide wavelength range undergoes a cyclic variation with a period of $\approx$5.5 yr. Most notable is the disappearance of the infrared (IR) emission line He I 10830 Å, which is referred to as a "spectroscopic event" (Damineli 1996). This is accompanied (albeit with some lag) by an observed flux density minimum at centimeter and millimeter wavelengths. While the cyclic flux density variations are usually attributed to the presence of a hot close binary companion, the influence of the highly unstable primary star is not yet understood (see Pittard 2003 for review).

The decrease in the measured SIMBA 1.2 mm flux densities from 2001 November to 2002 November follows the expected trend after the centimeter flux density maximum in 2000 (Duncan & White 2003; White 2005). SIMBA observations of η Car during the expected low-excitation phase in 2003 July yielded a 1.2 mm flux density minimum of 5 Jy (Abraham et al. 2005). Published 1.3 mm continuum data from the previous flux cycle, taken with the SEST over the period 1991–1996 (one measurement per year but not during the low-excitation phase), indicate a flux density minimum of 15.8 $\pm$ 1.9 Jy in 1992 and a flux density maximum of 38 $\pm$ 2 Jy in late 1995 (Cox 1997). On the basis of our SIMBA 2001/2002 1.2 mm data, it appears that the millimeter flux densities of η Car during the 1992.5–1998 and 1998–2003.5 cycles were similar. This is contrary to the flux density behavior at centimeter wavelengths, where the maximum 3 cm flux density reached in 2000 (1.7 Jy) was only 60% of the previous maximum in 1995 (2.9 Jy; Duncan & White 2003).

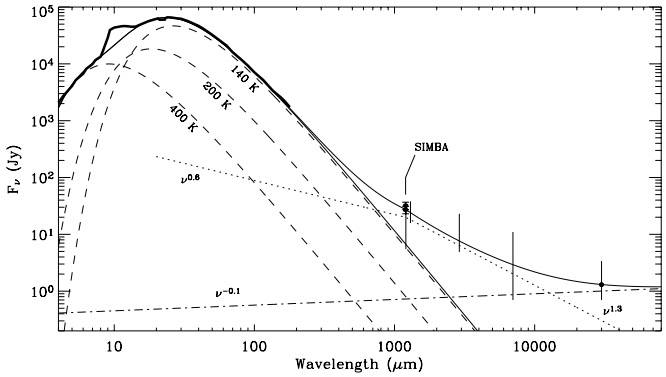

FIG. 3.—IR-to-radio spectral energy distribution of η Car showing a selection of data taken over the period 1992–2004 (spanning two 5.5 yr cycles). The 2–200 μm *ISO* spectrum (Morris et al. 1999) is shown by a thick line. The vertical bars show the range of flux densities measured at 1.2 and 7 mm (this work; Abraham & Damineli 1999; Abraham et al. 2005), 1.3 and 2.7 mm (Cox et al. 1995; Cox 1997), and 3 cm (White 2004). Note that the 1.3 and 2.7 mm data correspond to the 1992.5–1998 cycle only. A model has been fitted to the data that passes through our 2001/2002 1.2 mm SIMBA flux density range and the average 3 cm flux density during the same epoch (represented by a point). The model is composed of emission contributions from thermal dust from the Homunculus (dashed lines representing the 140, 200, and 400 K components), ionized circumstellar gas (*dot-dashed line*), plus the ionized stellar wind (dotted lines representing optically thin [$\nu^{0.6}$] and thick [$\nu^{1.3}$] components).

Figure 3 shows the IR-to-radio spectral energy distribution of η Car. This figure is an updated version of Figure 3 of Cox et al. (1995) and shows selected data taken over the period 1991–2004 (spanning two cycles). A model has been fitted to the data that is composed of contributions from thermal dust emission plus free-free emission coming from an ionized stellar wind component and an ionized circumstellar gas component.

For the shortest wavelengths, the 2–200 μm *Infrared Space Observatory* (*ISO*) spectrum, first presented by Morris et al. (1999), is fitted by three temperature components using the model by Smith et al. (2003b). In this model the 400 K component arises from hot dust close to the star. The 200 and 140 K components are primarily attributed to dust in the polar lobes of the neutral Homunculus nebula. More specifically, the 200 K component arises from warm dust at the inside of the lobes, whereas the 140 K component arises from cool dust in the outer walls. Since the bolometric luminosity does not change during a spectroscopic event, and because the dust is located far from the star, one would not expect the cool dust emission to vary much during the 5.5 yr cycle of η Car. However, the 10–20 μm variability has not been adequately studied.

The optically thin free-free radio emission that dominates at the longest wavelengths comes from ionized circumstellar gas condensations located within the Homunculus nebula and close to the star (Duncan & White 2003; White 2005). They are illuminated by variable amounts of ionizing UV radiation escaping from the putative central binary system during the 5.5 yr cycle. The most dramatic changes are seen in the high-excitation lines like He I and [Ne III] that respond to the hardest UV radiation, while low-excitation nebular lines show little variability (e.g., Gull et al. 2001).

It is clear from Figure 3 that the contribution from the ionized stellar wind of η Car is largest at millimeter wavelengths. The lowest 1.2 and 7 mm flux densities recorded in 2003 by Abraham et al. (2005) were the only time that millimeter flux densities were

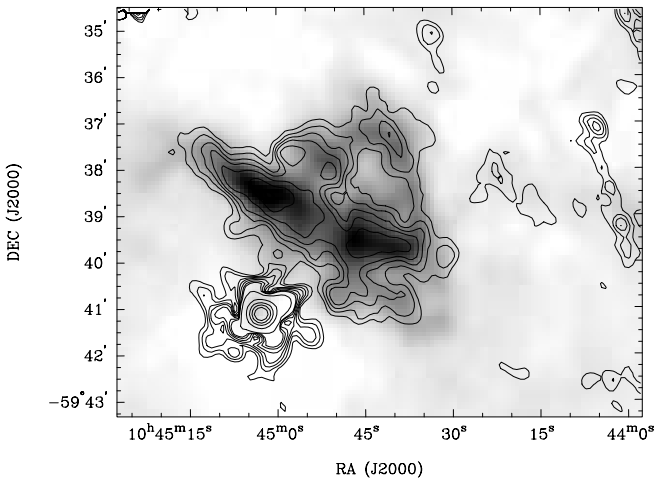

FIG. 4.—The 4.8 GHz continuum emission (Brooks et al. 2001) with contours of the SIMBA 1.2 mm continuum emission (see Fig. 1).

measured during a spectroscopic event. The value of the minimum 1.2 mm flux density is close to the expected contribution from cool dust in the Homunculus (140 K component), and the minimum 7 mm flux density is close to the expected contribution from the ionized circumstellar gas (extrapolated from the flux density minimum at 3 cm). This correspondence leads us to speculate that the millimeter emission from the ionized stellar wind of η Car completely shuts off during a spectroscopic event.

While there is little doubt that changes in the stellar wind of η Car dominate the flux density variability at millimeter wavelengths, it is not clear what the underlying physical process is that is regulating the changes. Cox (1997) and Cox et al. (1995) argue it is likely related to irregular mass-loss activity, regardless of the single or binary nature of the central star.

4.2. H II *Region*

The brightest emission from the H II region of the Keyhole nebula is associated with three well-defined radio-continuum components: Car II-E and Car II-W, both of which form a linear or barlike feature that extends over 5′ in the northeast-southwest direction, and Car II-N, which is in the shape of an arc. The 4.8 GHz flux densities of these three components are consistent with thermal free-free emission from ionization fronts originating from multiple early O-type stars in Tr 16 (Brooks et al. 2001). It is not known what is responsible for the striking ring-shaped morphology. Smith (2002) pointed out that the present-day polar axis of η Car appears to be aligned with the center of the ring and the break between Car II-E and Car II-W. The author argues that the highly bipolar stellar wind of η Car could easily have supplied the required momentum to puncture and inflate the Car II emission ring.

The total flux density of the 1.2 mm emission associated with Car II is 13 ± 2 Jy. This is comparable with the 1.3 mm flux density measurement by Cox et al. (1995) of 14 ± 4 Jy. The close spatial correlation between the 1.2 mm emission and the 4.8 GHz continuum emission (see Fig. 4) suggests that for these components the 1.2 mm emission arises from free-free emission associated with ionized gas and not, as is more often the case, cool dust emission associated with molecular gas. The lack of molecular line emission toward the Car II components (Cox & Bronfman 1995) supports this notion.

Brooks et al. (2001) measured peak flux densities at 4.8 GHz for Car II-N, Car II-W, and Car II-E of typically 0.07 Jy beam^{-1} with a HPBW of $8\farcs6 \times 6\farcs6$, implying brightness temperatures of $\approx$70 K. Assuming that the ionized gas has an electron temperature of 6000 K (Brooks et al. 2001), we estimate that the optical depth of the free-free emission at 4.8 GHz is $\sim$0.011. Since the optical depth and the brightness temperature in the optically thin regime both scale with frequency as $\nu^{-2.1}$, we expect the ionized gas to have an optical depth of 2.7×10^{-6} and a brightness of 1.6×10^{-2} K at 250 GHz (1.2 mm). The observed peak brightness at 1.2 mm (SIMBA with a HPBW of $24'' \times 24''$) of the Car II components are typically 1.2×10^{-2} K, in very good agreement with the expected value for thermal emission. We conclude that the 1.2 mm emission associated with the Car II radio components arises from thermal free-free emission.

Further confirmation of the nature of the 1.2 mm emission is found in the radio continuum spectrum for Car II shown in Figure 5. The data at 250 GHz (1.2 mm SIMBA) and 4.8 GHz (Brooks et al. 2001) were smoothed to match the beam size of the 0.843 GHz data ($43'' \times 50''$; Whiteoak 1994). Measurements for the flux density were obtained by integrating the flux over the total Car II emission source (an area defined by the 5 σ contour of the smoothed SIMBA data). The results are well fitted by the theoretical spectrum of a homogeneous constant density H II region using the formulae presented by Mezger & Henderson (1967).

4.3. *Molecular Globules*

Previous studies of the bright-rimmed dark globules apparent in the Hα image of Figure 2 have shown that they are molecular gas clumps with typical masses of order 10 $M_\odot$ and with photodissociation regions (PDRs) on their surfaces (Smith et al.

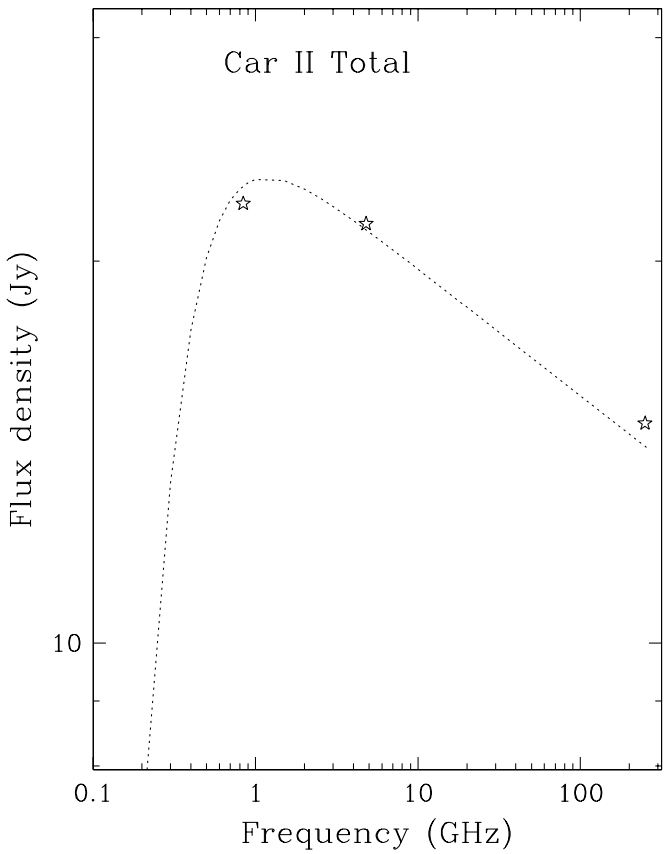

FIG. 5.—Radio continuum spectrum of Car II (total) using data at 0.843 GHz (Whiteoak 1994), 4.8 GHz (Brooks et al. 2001), and 250 GHz (this work). The dotted line corresponds to the best fit to the data using a theoretical model of a homogeneous region of ionized gas, $T_e = 6 \times 10^3$ K. Values for the fitted parameters are source size, $\theta = 192''$, and emission measure, EM = 2.1×10^5 pc cm^{-6}.

2004b; Rathborne et al. 2002; Brooks et al. 2000; Cox & Bronfman 1995). These molecular globules have characteristic sizes of a few tenths of a parsec and are being externally evaporated by the strong UV radiation field in the Carina nebula. They are analogous to small Bok globules like Thackeray's globules in IC 2944 (Thackeray 1950; Bok & Reilly 1947) and are probably the last remnants of the original cloud core from which Tr 16 formed.

All eight compact 1.2 mm emission sources identified in our SIMBA data (and listed in Table 1) overlap with these bright-rimmed molecular globules. Clump 5 is a prominent globule in Hα emission but is lost at 1.2 mm amid the bright emission from Car II-N. The 1.2 mm sources are either unresolved or just resolved by the SIMBA beam with approximate diameters of 40″ (0.4 pc). Column (7) of Table 1 lists the name of the molecular globule that matches each 1.2 mm source, and column (8) lists the corresponding mass estimate obtained from previous studies. These mass estimates have all been obtained from ^{12}CO(2–1) data (Cox & Bronfman 1995; Rathborne et al. 2002) except for clump 6, which relied on absorption of the He I λ10830 line (Smith 2002).

The overlap of the compact 1.2 mm sources with the molecular globules suggests that emission from dust is the predominant mechanism contributing to the 1.2 mm continuum emission. This is contrary to the case of the Car II emission ring, where thermal free-free emission is the dominant mechanism and no molecular line emission has been detected. Under this premise, we have used equation (1) to obtain mass estimates for each of the eight compact 1.2 mm emission clumps. On the basis of the work by Brooks et al. (2003) toward the PDR in the northern part of the Carina nebula, a value of $T_d = 45$ K was adopted. We assume $\kappa_{1.2} = 1$ cm^2 g^{-1}, as computed by Ossenkopf & Henning (1994) for typical conditions of dense protostellar clouds. For those clumps that are displaced from the Car II emission ring (clumps 6, 7, and 8), no 4.8 GHz continuum emission was detected with a 3 σ detection limit of 60 mJy. This translates to a maximum free-free flux contribution of 40 mJy at 1.2 mm for optically thin free-free emission and an additional mass uncertainty of $\approx$1 $M_\odot$. The resultant masses are listed in column (6) of Table 1. The values are in the range 3–19 $M_\odot$ and are in good agreement with the other mass estimates listed in Table 1. Clump 8 differs from the other clumps in that its mass estimate derived from molecular line data (Rathborne et al. 2002) is an order of magnitude larger than the dust derived mass and the mass of the other clumps.

A rather perplexing detail in the comparison of the Hα and 1.2 mm emission shown in Figure 2 is that the centers of the 1.2 mm compact sources do not match the darkest parts of the globules very well. Instead they match the bright Hα emission from the photoionized/photoevaporative flows coming off the globule surfaces. The apparent spatial distribution of the dust emission at 1.2 mm will be dominated by the relatively warm dust right behind the ionization fronts on the surfaces of the globules. Nevertheless, this does raise the concern that for some of the globules there may be a contribution to the 1.2 mm flux densities from free-free emission. However, the good agreement between the mass estimates from the 1.2 mm emission and molecular line emission and the absence of radio continuum emission implies that this contribution is minimal. Molecular line data at higher angular resolution toward the globules are needed in order to identify where the densest molecular gas is located for a detailed comparison.

4.4. *Dark Keyhole Structure*

The enigma of the dark keyhole structure dates back to 1830 and the first detailed drawings of the Keyhole nebula by Herschel, which show a keyhole shape that is somewhat different from today's picture. After much controversy about the reliability of Herschel's work, it is now generally accepted that the variations of the keyhole shape are real and were associated with the large luminosity fading of η Car after its bright phase from around 1822 to 1856 (see Viotti 1995 for a historical review). Evident in Figure 2 is the way in which the dark keyhole filaments pass in between the Car II-E and Car II-W emission. This stark superposition is yet to be explained and perhaps points to some sort of shadowing effect.

Cox & Bronfman (1995) detected molecular line emission toward the dark keyhole structure arising from three clumps (labeled clumps 1, 2, and 3 in their Fig. 1). Their observed and derived properties are similar to those of the other molecular clumps in the Keyhole nebula. In particular, their mass estimates from ^{12}CO (2–1) observations are 17, 11, and 4 $M_\odot$. However, unlike the other clumps, clumps 1, 2, and 3 show no bright Hα emission rims or PDR emission (absence of H_2 2.12 μm emission [Brooks et al. 2000] and PAH 3.3 μm [Rathborne et al. 2002]).

No 1.2 mm emission from the three molecular clumps of the dark keyhole structure was detected in our SIMBA data, which suggests that their temperatures are considerably smaller than the average temperature of the other clumps. For instance, for a clump of 10 $M_\odot$ and $T_d = 10$ K, we expect a flux density at 1.2 mm of 0.033 Jy, equivalent to the 2 σ observed detection limit. The absence of 1.2 mm emission supports the hypothesis (e.g., Brooks et al. 2000) that the dark keyhole structure is composed of cool ($T_d < 15$ K) foreground molecular clumps at the outskirts of the H II region.

It is possible that the three dark keyhole clumps provide a snapshot of an earlier phase of the bright-rimmed molecular globules in the nebula—before they were pressure-confined and were being externally photoevaporated by harsh UV radiation. This is supported by the fact that the keyhole clumps are bigger, more massive, darker, and more diffuse than the other clumps. Because of their proximity to the massive stellar members of Tr 16, the bright-rimmed globules are being photoevaporated, while for some reason the dark keyhole clumps are shielded. Interestingly, of all the bright-rimmed globules listed in Table 1, clumps A1 and A2 are bigger, more distorted looking, and more massive. Moreover, they are projected in almost the same place as the dark keyhole structure. We speculate that clumps A1 and A2 are younger, or at least less evolved, versions of the other bright-rimmed clumps and are in an earlier stage of being evaporated.

5. SUMMARY

The SIMBA 1.2 mm continuum data presented here highlight the complex nature of the Keyhole nebula and demonstrate the tremendous impact the nearby massive stars have had on the shaping of the region. We have detected 1.2 mm emission arising from free-free emission toward the bright ionized gas filaments known as the Car II radio continuum source, as well as emission from η Car. Numerous compact 1.2 mm emission sources have also been identified, which overlap with previously known bright-rimmed molecular globules. For these globules the 1.2 mm emission primarily arises from dust at $T_d \approx 45$ K. No 1.2 mm emission was detected from the three clumps of the dark keyhole structure, limiting their dust temperatures to $T_d < 15$ K.

The bright-rimmed molecular globules and the dark keyhole clumps are all that remain of the Carina GMC in the vicinity of the Keyhole nebula. They have been swept up from molecular gas by the stellar winds from η Car and are now being overrun to different degrees by ionization fronts. Perhaps the advancing ionization fronts will trigger radiation-driven implosion and the

molecular globules will become the sites of a new generation of star formation. There is building evidence to suggest that such triggered star formation is taking place elsewhere in the Carina nebula (e.g., Smith et al. 2000, 2004a; Rathborne et al. 2004). In a future paper we will present SIMBA 1.2 mm data covering the entire Carina nebula. These data have the potential to reveal emission peaks arising from embedded protostars and provide a census of a second generation of stars that have formed in a highly perturbed environment.

We thank the SEST staff for their support with the observations. K. J. B. and G. G. gratefully acknowledge support from the Chilean Centro de Astrofísica FONDAP 15010003.

REFERENCES

Abraham, Z., & Damineli, A. 1999, in ASP Conf. Ser. 179, Eta Carinae at the Millennium, ed. J. A. Morse, R. M. Humphreys, & A. Damineli (San Francisco: ASP), 263
Abraham, Z., Falceta-Gonçalves, D., Dominici, T. P., Nyman, L.-Å., Durouchoucx, P., McAuliffe, F., Caproni, A., & Jatenco-Pereira, J. 2005, A&A, 437, 977
Allen, D. A., & Hillier, D. J. 1993, Publ. Astron. Soc. Australia, 10, 338
Bok, J. B., & Reilly, E. F. 1947, ApJ, 105, 255
Brooks, K. J., Burton, M. G., Rathborne, J. M., Ashley, M. C. B., & Storey, J. W. V. 2000, MNRAS, 319, 95
Brooks, K. J., Cox, P., Schneider, N., Storey, J. W. V., Poglitsch, A., Geis, N., & Bronfman, L. 2003, A&A, 412, 751
Brooks, K. J., Storey, J. W. V., & Whiteoak, J. B. 2001, MNRAS, 327, 46
Brooks, K. J., Whiteoak, J. B., & Storey, J. W. V. 1998, Proc. Astron. Soc. Australia, 15(2), 202
Chini, R., Krugel, E., & Wargau, W. 1987, A&A, 181, 378
Chini, R., et al. 2003, A&A, 409, 235
Cox, P. 1997, in ASP Conf. Ser. 120, Luminous Blue Variables: Massive Stars in Transition, ed. A. Nota & H. J. G. L. M. Lamers (San Francisco: ASP), 277
Cox, P., & Bronfman, L. 1995, A&A, 299, 583
Cox, P., Mezger, P. G., Sievers, A., Najarro, F., Bronfman, L., Kreysa, E., & Haslam, G. 1995, A&A, 297, 168
Damineli, A. 1996, ApJ, 460, L49
Duncan, R. A., & White, S. M. 2003, MNRAS, 338, 425
Gardner, F. F., & Morimoto, M. 1968, Australian J. Phys., 21, 881
Gull, T. R., Ishibashi, K., Davidson, K., & Collins, N. 2001, in ASP Conf. Ser. 242, Eta Carinae and Other Mysterious Stars: The Hidden Opportunities of Emission Spectroscopy, ed. T. R. Gull, S. Johannson, & K. Davidson (San Francisco: ASP), 391
López, J. A., & Meaburn, J. 1986, Rev. Mex. AA, 13, 27
Mezger, P. G., & Henderson, A. 1967, ApJ, 147, 471
Morris, P. W., et al. 1999, Nature, 402, 502
Ossenkopf, V., & Henning, T. 1994, A&A, 291, 943
Pittard, J. 2003, Astron. Geophys., 44(1), 1.17
Rathborne, J. M., Brooks, K. J., Burton, M. G., Cohen, M., & Bontemps, S. 2004, A&A, 418, 563
Rathborne, J. M., Burton, M. G., Brooks, K. J., Cohen, M., Ashley, M. C. B., & Storey, J. W. V. 2002, MNRAS, 331, 85
Reichertz, L. A., Weferling, B., Esch, W., & Kreysa, E. 2001, A&A, 379, 735
Smith, N. 2002, MNRAS, 331, 7
Smith, N., Bally, J., & Brooks, K. J. 2004a, AJ, 127, 2793
Smith, N., Bally, J., & Morse, J. A. 2003a, ApJ, 587, L105
Smith, N., Barbá, R. H., & Walborn, N. R. 2004b, MNRAS, 351, 1457
Smith, N., Egan, M. P., Carey, S., Price, S. D., Morse, J. A., & Price, P. A. 2000, ApJ, 532, L145
Smith, N., Gehrz, R. D., Hinz, P. M., Hoffmann, W. F., Hora, J. L., Mamajek, E. E., & Meyer, M. R. 2003b, AJ, 125, 1458
Thackeray, A. D. 1950, MNRAS, 110, 343
Viotti, R. 1995, in Rev. Mex. AA Ser. Conf. 2, The Eta Carinae Region: A Laboratory of Stellar Evolution, ed. V. Niemela, N. Morrell, & A. Feinston (Mexico: UNAM), 1
Walborn, N. R., & Liller, M. H. 1977, ApJ, 211, 181
White, S. M., Duncan, R. A., Chapman, J. M., & Koribalski, B. 2005, in ASP. Conf. Ser. 332, The Fate of the Most Massive Stars, ed. R. M. Humphreys (San Francisco: ASP), 126
Whiteoak, J. B. Z. 1994, ApJ, 429, 225